Ideal mean-field transition in a modulated cold atom system

Myoung-Sun Heo,[1] Yonghee Kim,[1] Kihwan Kim,[1] Geol Moon,[1] Junhyun Lee,[1] Heung-Ryoul Noh,[2] M. I. Dykman,[3,*] and Wonho Jhe[1,†]

[1]*Department of Physics and Astronomy, Seoul National University, Seoul 151-747, Korea*
[2]*Department of Physics, Chonnam National University, Gwangju 500-757, Korea*
[3]*Department of Physics and Astronomy, Michigan State University, East Lansing, Michigan 48824, USA*
(Received 5 January 2010; revised manuscript received 9 March 2010; published 24 September 2010)

We show that an atomic system in a periodically modulated optical trap displays an ideal mean-field symmetry-breaking transition. The symmetry is broken with respect to time translation by the modulation period. We describe experimental observations and develop a full microscopic theory of the observed critical phenomena. The transition is explained as resulting from the interplay of the long-range interatomic interaction and nonequilibrium fluctuations in the strongly modulated system. The observations, including anomalous fluctuations in the symmetry broken phase, are fully described by the theory.

DOI: 10.1103/PhysRevE.82.031134 PACS number(s): 05.70.Fh, 05.40.−a, 05.70.Ln, 67.85.−d

I. INTRODUCTION

The mean-field approach has been instrumental for developing an insight into symmetry-breaking transitions in thermal equilibrium systems [1]. It has been broadly applied also to nonequilibrium systems, the studies of pattern formation being an example [2]. However, close to the phase-transition point the mean field approximation usually breaks down. This happens even in finite-size systems provided they are sufficiently large.

In this paper we study a nonequilibrium system of $\sim 10^7$ particles which, as we show, displays an ideal mean-field symmetry-breaking transition. It is accompanied by anomalous fluctuations, which are also described by an appropriately extended mean-field theory. The system is formed by moderately cold atoms in a magneto-optical trap (MOT) in the classical regime [3,4]. The atoms are periodically modulated in time [5].

Periodically modulated systems form one of the most important classes of nonequilibrium systems, both conceptually and in terms of applications. They have discrete time-translation symmetry: they are invariant with respect to time translation by modulation period τ_F. Nevertheless, they may have stable vibrational states with periods that are multiples of τ_F, in particular $2\tau_F$. Period doubling is well known from parametric resonance, where a system has two identical vibrational states shifted in phase by π. It is broadly used in classical and quantum optics and has attracted significant attention recently in the context of nano- and micromechanical resonators [6–9].

It should be emphasized that, in a many-body system, dynamical period doubling in itself does *not* break the time-translation symmetry. This is a consequence of fluctuations. Even though each vibrational state has a lower symmetry, fluctuations make the states equally populated and the system as a whole remains symmetric. However, if as a result of the interaction the state populations become different, the symmetry is broken. It is reminiscent of the Ising transition where the interaction leads to preferred occupation of one of the two equivalent spin orientations, except that the symmetry is broken in time. For atoms in a parametrically modulated MOT spontaneous breaking of the discrete time-translation symmetry was observed experimentally by Kim *et al.* [10].

Here we show that the time-translation symmetry breaking in a modulated MOT results from the cooperation and competition between the interparticle interaction and the fluctuations that lead to atom switching between the vibrational states. The interaction has a long-range part, but is weak. On its own, it cannot change the state populations. However, it may change the rates of fluctuation induced switching, which in turn will cause the population change. We provide a quantitative theory of the phenomenon. We measure the critical exponents and the frequency dispersion of the susceptibility. The observations are consistent with the mean-field behavior and are in good agreement with the theory.

The paper is organized as follows. In Sec. II, we describe the experimental observations and provide a brief outline of the theory. The full theory is described in the remainder of the paper. In Sec. III, we develop a theory of intercloud switching. We consider the effect of the interatomic coupling on the switching rates and show that, even far from thermal equilibrium, it can be described in simple and general terms. In Sec. IV, we use the results on the switching rates to describe the spontaneous breaking of the discrete time-translation symmetry. We obtain the critical exponents, including the exponent pertaining to the nonlinear response to a resonant high-frequency field at the transition point; we also find the spectrum of the response to a nearly resonant field. In Sec. V, we explain anomalous critical fluctuations due to atom evaporation and recapture into the trap. Section VI provides explicit results for a simple model of one-dimensional (1D) motion. The shadow effect in the rotating frame is described. It is argued that the corresponding interaction is responsible for the symmetry-breaking transition. Section VII contains concluding remarks.

*dykman@pa.msu.edu
†whjhe@snu.ac.kr

II. EXPERIMENTAL RESULTS AND A PREVIEW OF THE THEORY

A. Experimental setup

In the experiment, ^{85}Rb atoms in a MOT were cooled down to ≈ 0.4 mK. Full three-dimensional confinement was achieved with three pairs of counterpropagating laser beams. The intensity of the beams along the MOT axis z was 0.19 mW/cm^2, the transverse beam intensities were five to ten times larger. The magnetic field gradient at the trap center was 10 G/cm. The transverse beams were detuned from the atomic transition by $\delta \approx -2.3\Gamma_p$, the longitudinal beams were further detuned by 5 MHz (the atomic decay rate is $\Gamma_p/2\pi \approx 5.9$ MHz). The atomic cloud motion was essentially one-dimensional, along z axis, with frequency $\omega_0/2\pi \approx 45$ Hz and the damping rate $\Gamma \approx 36$ s^{-1}. The total number of trapped atoms N_{tot} was varied by changing the hyperfine-repumping laser intensity at a decrease rate of 0.5% per second. For the order parameter and the variance measurements very close to criticality, the decrease rate was reduced to 0.03%.

The beam intensities were modulated at frequency $\omega_F = 2\omega_0$ by acousto-optic modulators. When the modulation amplitude exceeded a threshold value, after a transient, the atomic cloud split into two clouds [5], which were vibrating in counterphase with frequency $\omega_F/2$, see Fig. 1(a). We took snapshots at the maximum separation of the clouds at the frame rate of 1–50 Hz to obtain the population of each cloud. For a small total number of trapped atoms N_{tot} the populations were equal and the cloud vibrations had equal amplitudes. This shows that the system as a whole preserved the symmetry with respect to time translation by the modulation period.

Once N_{tot} exceeded a critical value N_c ($N_c \sim 10^7$ in our experiment), the average populations of the clouds became different, as observed earlier [10]. We observe that the vibration amplitudes become different, too, see Fig. 1(b). This is spontaneous breaking of the discrete time-translation symmetry, the system becomes invariant with respect to time translation by $2\tau_F$, not the modulation period τ_F.

B. Mechanism of the symmetry breaking

As phase transitions in equilibrium systems, the observed transition is a many-body effect. This is evidenced by the required critical number of atoms, which is finite but large, typical of phase transitions in quantum cold atom systems [11–15]. In contrast to these systems, atomic dynamics in our system is classical. More importantly, the system is far from thermal equilibrium, it is not characterized by the free energy and has a discrete time-translation symmetry. Remarkably, there are no long-range correlations of spatial density fluctuations. The intracloud density fluctuations are irrelevant, they are uncorrelated with the intercloud fluctuations, which, as we show, are responsible for the transition and display critical slowing down. As a result, the symmetry breaking is quantitatively described by the mean-field theory.

The mean-field behavior is ultimately rooted in the time scale separation and the weakness of the interaction. The

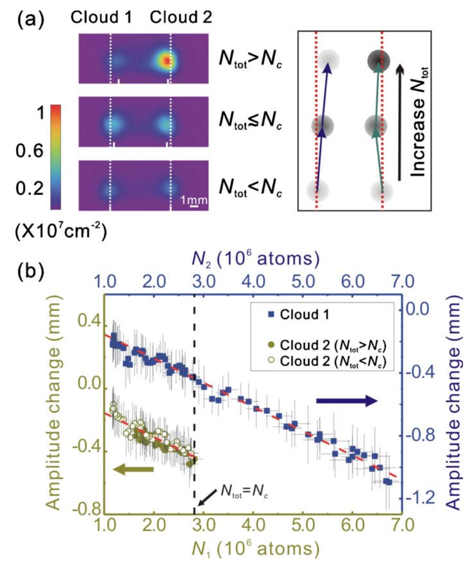

FIG. 1. (Color online) (a) The two-dimensional density profiles of the vibrating clouds for the maximal displacement along the MOT axis (≈ 4.5 mm). The lower, middle, and upper panels refer to the symmetric, close to critical, and broken-symmetry states, with $N_{\mathrm{tot}} \approx 1.5 \times 10^6$, 5.2×10^6, and 6.7×10^6, respectively; $N_c \approx 5.6 \times 10^6$. The cloud centers are indicated by the ticks at the bottom of the panels and are sketched in the right panel. (b) Cloud vibration amplitudes as functions of the population of the other cloud as it changes with the increasing N_{tot}. The (tilted) red dashed lines show the expected linear dependence, cf. Equation (37). The vertical dashed line shows $N_1 = N_2 = N_c/2$. For the cloud with smaller population beyond the transition, cloud 1, the amplitude monotonically increases with N_{tot}, whereas for the larger cloud, cloud 2, the amplitude is maximal at criticality. The error bars show the standard deviation for 20 measurements.

decay of correlations of intracloud density fluctuations is characterized by the damping rate Γ of atomic motion, which is determined by the Doppler effect in the MOT [4] and does not change at the phase transition. On the other hand, switching between periodic states generally requires a large fluctuation and involves overcoming an effective activation barrier [8,16–20]. For low temperature, switching is a rare event. We measured the rates W_{nm} of intercloud $n \to m$ switching $(n,m=1,2)$ directly for small N_{tot} from the decay time of the difference of the cloud populations, which gave $W_{12} = W_{21} \sim 1$ s^{-1}. Therefore, in the experiment there is a strong inequality between the characteristic reciprocal times,

$$\omega_F \gg \Gamma \gg W_{nm}. \tag{1}$$

This inequality shows, in particular, that the number of atoms in each cloud remains almost constant over the period, even though the cloud shapes can vary, for nonsinusoidal vibrations.

During switching an atom is far from the clouds. The energy of its interaction with individual atoms in the clouds is much smaller than k_BT. However, the total energy of interaction with *all* atoms in the clouds may exceed k_BT, and then it changes the intercloud switching rate. The interaction depends on the individual cloud populations $N_{1,2}$ and the

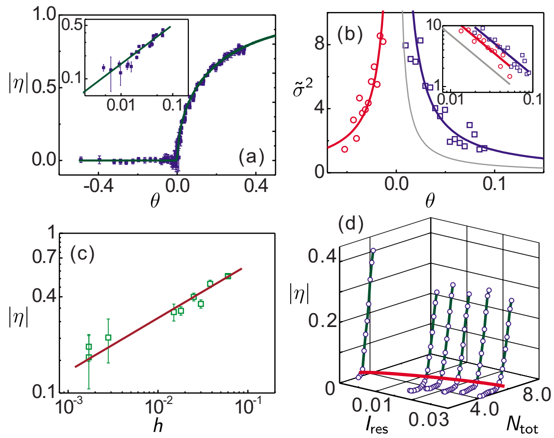

FIG. 2. (Color online) (a) The relative difference of the cloud populations $\eta = \langle N_2 - N_1 \rangle / N_{tot}$ as a function of the control parameter $\theta = (N_{tot} - N_c)/N_c$; the critical total number of trapped atoms N_{tot} is $N_c = 1.6 \times 10^7$. The solid curves show the mean-field theory, $\eta = \tanh[(\theta+1)\eta]$. In the experiment $|\eta| \propto \theta^\beta$ with $\beta = 0.51 \pm 0.01$ for $0 < \theta \ll 1$ (inset). (b) The variance of the order parameter $\tilde{\sigma}^2 = 10^3 \sigma^2$ and its scaling (inset). The critical exponents in the symmetric and broken-symmetry phases are, respectively, $\tilde{\gamma} = 1.04 \pm 0.21$ and $\tilde{\gamma} = 1.11 \pm 0.13$. The gray line shows the theoretical result in the absence of fluctuations of N_{tot}. (c) The order parameter at criticality ($\theta = 0$) as a function of amplitude h of the additional modulation at frequency $\omega_F/2$; h is scaled by the strong modulation amplitude. The solid line is $|\eta| \propto h^{1/\delta}$, with $\delta = 3$; experimentally, $\delta = 3.0 \pm 0.8$. (d) Order parameter $|\eta|$ as a function of N_{tot} (in units of 10^7 atoms) and the intensity of the additional resonant radiation (scaled by the saturation intensity, 3.78 mW/cm^2). The red curve in the (I_{res}, N_{tot}) plane is the phase-transition line. The error bars in panels (a) and (c) show the standard deviations of ten measurements.

density distribution within the clouds, which changes only weakly with N_{tot}.

The switching rates modification by the atom-atom interaction is the underlying mechanism of the symmetry breaking. Since these are the cloud populations $N_{1,2}$ that control the switching rates and that are changed as a result of switching, we choose their mean relative difference $\eta = \langle N_2 - N_1 \rangle / N_{tot}$ as the order parameter. A natural control parameter is the reduced total number of atoms $\theta = (N_{tot} - N_c)/N_c$. For the symmetry breaking to occur, the interaction should correspond to the effective attraction between the vibrating clouds. As we show, an appropriate interaction is provided by the shadow effect in the trap [3,4,21–23].

C. Experimental observations

Our main observations are presented in Figs. 2 and 3. They show that all measured quantities display mean-field critical behavior. The order parameter scales as $|\eta| \propto \theta^\beta$ for $\theta > 0$, with $\beta \approx 1/2$, see Fig. 2(a), and $\eta = 0$ for $\theta < 0$. This scaling was also seen earlier [10], but now we have come much closer to the critical point, and the precision is much higher.

In Fig. 2(b), we show the results on the variance of fluctuations of the population difference, $\sigma^2 = N_{tot}^{-2} \langle (N_2 - N_1)^2 \rangle - \eta^2$. We find that it scales as $\sigma \propto |\theta|^{-\tilde{\gamma}}$ with $\tilde{\gamma} \approx 1$ for positive and negative θ.

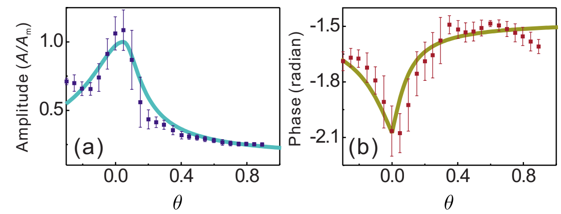

FIG. 3. (Color online) The amplitude (a) and phase (b) of oscillations of the order parameter η induced by an extra modulation at frequency $\omega_F/2 + \Omega$ with $\Omega = 0.1$ Hz; in (a), the amplitude is scaled by its value A_m for $\theta = 0$. The solid curves show the theory, Eq. (22), with the $N_{tot} \to 0$ switching rate used as a fitting parameter. The error bars show the standard deviations of 100 measurements.

Equilibrium systems at criticality show a strongly nonlinear response to the symmetry-breaking static field, like a magnetic field at the Ising transition. For our system an analog of such field is an additional periodic driving at half the strong-field frequency. With this field, the overall time-translation period is $2\tau_F$, and the vibrational states of period $2\tau_F$ become nonequivalent [24]. We studied the effect of the dynamic symmetry-breaking field at criticality, $\theta = 0$, by asymmetrically modulating the counterpropagating beams. Figure 2(c) shows that the cloud population difference scales with the additional field amplitude h as $|\eta| \propto h^{1/\delta}$ with $\delta \approx 3$, in agreement with the mean field theory.

The critical slowing down should lead to a strong response of the population difference to a field detuned by a small frequency Ω from $\omega_F/2$. This is an analog of applying a weak slowly varying field to thermal equilibrium systems. The amplitude and phase of the forced oscillations of η at frequency Ω as functions of θ are shown in Fig. 3. They display characteristic asymmetric resonant features, again in excellent agreement with the mean-field theory.

D. Summary of the theoretical results

In general, one should not expect that our oscillating system can be described by the Landau-type theory with standard critical exponents, and in fact the theory has to be extended. We explain the observations as due to kinetic many-body effects. They turn out to be strong as a consequence of the exponential sensitivity of the intercloud switching rates W_{nm}.

If the atom-atom coupling can be disregarded, the switching rates are equal by symmetry,

$$W_{12}^{(0)} = W_{21}^{(0)} \equiv W^{(0)} = C_W \exp(-R^{(0)}/k_B T) \qquad (2)$$

with $C_W \sim \omega_{cl}$, where ω_{cl} is the frequency of small-amplitude damped atom vibrations about the cloud center (in the experiment, $\omega_{cl} \approx 3\Gamma$). Of primary interest is the activation energy $R^{(0)}$. For weakly nonsinusoidal period-2 vibrations it was calculated and measured for single-oscillator systems with cubic nonlinearity [8,16,17]. If we use the same model, for the present experimental parameters, the theory [16] gives $R^{(0)}/k_B \approx 3.4$ mK. This is within a factor of 2 of the value extracted from the measured $W^{(0)}$ and estimated T, which is satisfactory given that in the present case the parametric modulation was comparatively strong and therefore the vibrations were noticeably nonsinusoidal (the squared MOT eigenfrequency ω_0^2 was modulated with relative amplitude 0.9).

The atom-atom interaction changes the switching activation energy. The change becomes significant only because of the cumulative effect of the interaction of a switching atom with the atoms in the clouds. We emphasize the distinction from the standard Ising model with global coupling: not only is our system far from equilibrium, but the atom-atom interaction is not $\propto 1/N_{\rm tot}$. Symmetry-breaking occurs with increasing $N_{\rm tot}$, and even though the system is large, obviously there is no thermodynamic limit $N_{\rm tot}\to\infty$.

For not too strong interaction the rate of $1\to 2$ switching becomes

$$W_{12}(N_1;N_{\rm tot}) = W^{(0)} \exp[-2\alpha N_1 + (\alpha+\beta)N_{\rm tot}], \qquad (3)$$

see Sec. III; the rate of $2\to 1$ switching is given by the same expression with $N_1\leftrightarrow N_2$. The parameters α,β are $\propto 1/T$, see Eq. (9), which shows that the effect of the interaction increases with decreasing temperature; on the other hand, without noise the weak interaction would only weakly perturb the system and there would be no symmetry-breaking transition. We will be interested in the effectively attractive interaction between atoms in different clouds, for which $\alpha>0$.

The probability P_1 to have N_1 atoms in cloud 1 for given $N_{\rm tot}$ can be found from the balance equation. For $N_{\rm tot}\gg 1$, the stationary probability $P_1^{\rm st}(N_1)$ is a function of the reduced population difference $x=(N_2-N_1)/N_{\rm tot}$ and the control parameter $\theta=\alpha N_{\rm tot}-1$. It has a sharp maximum whose position gives the order parameter $\eta=\langle x\rangle$.

For fixed $N_{\rm tot}$, near criticality ($|x|,|\theta|\ll 1$) the stationary distribution has a characteristic Landau mean-field form [25], $P_1^{\rm st}\propto\exp[-N_{\rm tot}(x^4-6\theta x^2)/12]$, see Eq. (12). For $\theta<0$ it has a peak at $x=\eta=0$, which corresponds to equal mean cloud populations. For $\theta>0$ and $|\theta|\gg N_{\rm tot}^{-1/2}$ the symmetry is broken and $\langle x\rangle=\eta=\pm(3\theta)^{1/2}$. This describes the dependence of η on θ in Fig. 2(a). The form of $P_1^{\rm st}$ explains also the scaling $\sigma^2\propto|\theta|^{-1}$ of the variance $\sigma^2=\langle x^2\rangle-\langle x\rangle^2$ in Fig. 2(b).

The critical total number of atoms (where $\theta=0$) is $N_c=\alpha^{-1}$. Thus, $N_c\propto T$. This dependence was tested by heating up the atoms with additional resonant radiation. Indeed, N_c was found to increase almost linearly with the radiation intensity, see Fig. 2(d).

An extra modulation of the beam intensities $h\cos(\omega_F t/2+\phi_h)$ leads to factors $\exp(h_{12})$ and $\exp(-h_{12})$ in the switching rates W_{12} and W_{21}, with $h_{12}\propto h/T$ [24]. In calculating these factors one can disregard the weak atom-atom interaction. As a result, $P_1^{\rm st}$ is multiplied by $\exp(N_{\rm tot}h_{12}x)$, Eq. (17). This gives $\eta\propto h^{1/3}$ at criticality ($\theta=0$), in agreement with the experiment. If the frequency of the extra modulation is slightly detuned from $\omega_F/2$, the linear response does not diverge at criticality. The result of the calculation in Sec. IV is in excellent agreement with the experiment, as seen from Fig. 3.

An independent estimate of the interaction strength can be obtained from the dependence of the vibration amplitudes of the clouds on the cloud populations. For comparatively weak interaction, the interaction-induced change of the amplitude of an nth cloud should be proportional to the number of atoms in the other cloud $N_{3-n}(n=1,2)$. This is indeed seen in Fig. 1(b). The main contribution comes from the long-range interaction, the shadow effect [4,21,22]. This interaction also gives the main contribution to the parameters α,β and thus determines the critical total number of atoms N_c. The value of N_c obtained in a simple one-dimensional model that assumes sinusoidal vibrations, Sec. VI, is within a factor of 2 from the experimental data, as are also the slopes of the straight lines in Fig. 1(b).

In the experiment, the total number of trapped atoms was slowly fluctuating. The mean-field theory still remains applicable, but needs to be extended, see Sec. V. An important consequence is that in the symmetric phase the variance does not change, $N_c\sigma^2=|\theta|^{-1}$, whereas in the low-symmetry phase, $1\gg\theta\gg N_c^{-1/2}$, the variance is modified, $N_c\sigma^2=(2\theta)^{-1}+3(4\theta+\varepsilon)^{-1}$, where $\varepsilon=W_{\rm out}/[W^{(0)}\exp(\beta N_c)]$, $\varepsilon\ll 1$, see Eq. (27); here, $W_{\rm out}$ is the probability for an atom to leave the trap per unit time. The variance is larger than in the symmetric phase for the same $|\theta|$ by factor 5/4 for $\theta\gg\varepsilon$ and is smaller by factor 2 for smaller θ, i.e., closer to N_c where fluctuations of $N_{\rm tot}$ are averaged out [see the gray line in Fig. 2(b)]. The scaling $\sigma^2\propto\theta^{-1}$ holds in the both limits. This is the scaling seen in Fig. 2(b). In the experiment, it was not possible to come close enough to N_c to observe the crossover; σ^2 in the broken-symmetry phase remained larger than in the symmetric phase.

III. THEORY OF INTERCLOUD SWITCHING

A. Single-atom switching

We now provide a full theory of the critical phenomena in a parametrically modulated MOT. We start with the single-atom dynamics for the modulation frequency ω_F close to twice the eigenfrequency ω_0 of atomic vibrations in the MOT. The modulation can lead to the onset of period-two vibrations at frequency $\omega_F/2$. These vibrations are close to sinusoidal for moderately strong modulation, there is no dynamical chaos in the range of phase space of interest. In the single-atom approximation the equation of motion can be written as

$$m_a\ddot{\mathbf{r}} = \mathbf{G}(\mathbf{r},\dot{\mathbf{r}};t) + \mathbf{f}(t), \qquad (4)$$

where $\mathbf{r}$ is the position vector of an atom, m_a is the atomic mass, and $\mathbf{G}$ is the well-understood force from the laser beams [4,23,26]; for modulated beams it periodically depends on time, $\mathbf{G}(t+\tau_F)=\mathbf{G}(t)$. The force $\mathbf{f}(t)$ in Eq. (4) is the zero-mean noise from spontaneous light emission. Often the friction force in $\mathbf{G}$ is assumed to have the form $-2\Gamma m_a\dot{\mathbf{r}}$, where Γ is the effective friction coefficient; then the noise is modeled by white Gaussian noise,

$$\langle f_\kappa(t)f_{\kappa'}(t')\rangle = 4\Gamma m_a k_B T\delta_{\kappa\kappa'}\delta(t-t'),$$

where T is the characteristic gas temperature, and $\kappa,\kappa'=x,y,z$ enumerate the atomic coordinates.

We are interested in the parameter range where, in the absence of noise, Eq. (4) has two stable periodic solutions

$\mathbf{r}_{1,2}(t)$, with $\mathbf{r}_n(t+2\tau_F)=\mathbf{r}_n(t)(n=1,2)$ and $\mathbf{r}_2(t)=\mathbf{r}_1(t+\tau_F)$. These solutions give the positions of the centers of the vibrating atomic clouds, cf. Fig. 1(a). By linearizing Eq. (4) about $\mathbf{r}_n(t)$ one finds the typical frequencies $\omega_{\rm cl}$ and relaxation rates ($\sim\Gamma$) of the intracloud motion. Noise leads to fluctuations about $\mathbf{r}_n(t)$ with variance $\propto T$ that determines the size of the clouds in Fig. 1.

Switching between the clouds results from large rare fluctuations. It is central for the analysis that the switching rates are much smaller than ω_F and than $\omega_{\rm cl},\Gamma$. Therefore of interest are period-averaged rates W_{nm} of $n\to m$ switching, $n,m=1,2$. Quite generally [27,28]

$$W_{nm}=C_W\exp(-R_n/k_BT), \tag{5}$$

where the prefactor $C_W\sim\max(\omega_{\rm cl},\Gamma)$. The most important in W_{nm} is the exponential factor, which has the activation form. The activation energy R_n of switching from the periodic state n is given by the solution of a variational problem $R_n=\min\mathcal{R}$, where the functional $\mathcal{R}$ is [28],

$$\mathcal{R}=(8\Gamma m_a)^{-1}\int dt\mathbf{f}(t)^2+\int dt\boldsymbol{\lambda}(t)[m_a\ddot{\mathbf{r}}-\mathbf{G}-\mathbf{f}(t)]. \tag{6}$$

Here, the term quadratic in $\mathbf{f}$ determines the probability density of a realization of the random force that leads to switching [29]; $\boldsymbol{\lambda}(t)$ is the Lagrange multiplier that relates the dynamics of the atom and the force to each other. For switching from nth periodic state, the trajectory $\mathbf{r}(t)$ should go from $\mathbf{r}_n(t)$ for $t\to-\infty$ to the unstable periodic saddle-type state $\mathbf{r}_b(t)$ on the boundary of the basin of attraction to $\mathbf{r}_n(t)$ for $t\to\infty$; $\boldsymbol{\lambda}(t),\mathbf{f}(t)\to\mathbf{0}$ for $t\to\pm\infty$.

Since in the single-atom case the period-two vibrational states differ only by phase, the activation energies $R_{1,2}$ are equal, $R_1=R_2=R^{(0)}$. The variational problem is significantly simplified if the vibrations $\mathbf{r}_n(t)$ are almost sinusoidal, which corresponds to small damping and comparatively weak nonlinearity, see Sec. VI.

B. Switching rate modification by the atom-atom interaction

The interaction between atoms leads to an extra force $\mathbf{G}_{\rm int}(\mathbf{r})$ in Eq. (4). This force is weak in the sense that it weakly affects the intracloud atomic dynamics. In the experiment, the radius of the clouds changed by $\sim10\%$ where the number of atoms changed by a factor of 2. The change of the vibration amplitude was also small, see Fig. 1.

The force $\mathbf{G}_{\rm int}$ depends on the positions of all atoms. It can be separated into the mean-field and fluctuating parts. The mean-field part is due to the long-range interaction [4]. The fluctuating part is dominated by short-range elastic collisions. For comparatively low atomic densities and high temperatures used in the experiment the effect of the fluctuating part of $\mathbf{G}_{\rm int}$ is small compared to that of the thermal noise and will be disregarded.

Of primary interest to us is the intercloud interaction and the effect of the interaction on the atoms switching between the clouds. This effect is determined by the long-range part of the interaction and can be described in terms of the mean-field force. Indeed, since on average the interatomic distance in the cloud is small compared to the distance to the switching atom or to the other cloud, the force $\mathbf{G}_{\rm int}$ depends on the intracloud atomic density, individual atoms are not "resolved." This is further strengthened by the fact that short-range (of the order of the interatomic distance) density fluctuations in the clouds are very fast, with correlation time $\sim\omega_{\rm cl}^{-1}N_{\rm tot}^{-1/3}\ll\Gamma^{-1}$, and therefore are averaged out.

From the above arguments, the long-range force on an atom $\mathbf{G}_{\rm int}(\mathbf{r})$, can be written as

$$\mathbf{G}_{\rm int}(\mathbf{r})=\sum_{m=1,2}N_m\mathbf{G}_{\rm int}(\mathbf{r};m), \tag{7}$$

where N_m is the number of atoms in cloud m. The force $\mathbf{G}_{\rm int}(\mathbf{r};m)$ is determined by the density distribution in the cloud m.

Even though $\mathbf{G}_{\rm int}$ is small compared to the overall force on an atom $\mathbf{G}$, it may strongly affect the switching rate, leading to the spontaneous symmetry breaking. This is because $\mathbf{G}_{\rm int}$ changes the switching activation energy R_n. Extending to the many-atom system the approach of Ref. [30], (the justification is given below), to first order in the interaction we obtain $R_n=R^{(0)}+R_n^{(1)}$ with

$$R_n^{(1)}=\sum_m\alpha_{nm}N_m,$$

$$\alpha_{nm}=-\int_{-\infty}^{\infty}dt\boldsymbol{\lambda}_n^{(\rm opt)}(t)\mathbf{G}_{\rm int}(\mathbf{r}_n^{(\rm opt)}(t);m). \tag{8}$$

Here, $\mathbf{r}_n^{(\rm opt)}(t)$ and $\boldsymbol{\lambda}_n^{(\rm opt)}(t)$ describe the trajectory that minimizes functional $\mathcal{R}$, Eq. (6), for switching from periodic state n (i.e., from nth cloud). Function $\mathbf{r}_n^{(\rm opt)}(t)$ gives the most probable path followed in the switching; for a parametrically excited oscillator this path has been observed in experiment [31]. Since the states 1 and 2 differ only in phase, we have $\alpha_{11}=\alpha_{22}$ and $\alpha_{12}=\alpha_{21}$.

In deriving Eq. (8) we used that, first, because the interatomic interaction is weak, atoms switch one by one, not in groups; switchings of individual atoms are uncorrelated. Second, and most importantly, in the optimal fluctuation leading to switching of an atom the atomic clouds practically do not change their shape. This is also a consequence of the interatomic interaction being weak: the force from a single atom in the cloud very weakly affects the motion of the switching atom, $|\alpha_{nm}|\ll k_BT$, and vice versa, the force from the switching atom on the atoms in the cloud is weak. Only the effect from all atoms in the cloud on a switching atom is appreciable, the product $\alpha_{nm}N_m$ ($N_{1,2}\gg1$) can become larger than k_BT.

A significant change of the shapes of the clouds, even though it would change the switching activation energy, has an exceedingly small probability. Indeed, if the cloud radius is $a_0\sim(k_BT/m_a\omega_{\rm cl}^2)^{1/2}$, the probability density to have the atoms in nth cloud displaced by $\Delta r_n\gg a_0$ is $\propto\exp(-N_n\Delta r_n^2/2a_0^2)\ll1$. At the same time, the change of α_{nm} would be proportional to the ratio of Δr_n to the characteristic intercloud distance, which is of the order of the vibration amplitude and largely exceeds a_0. Therefore in calculating $\mathbf{G}_{\rm int}(\mathbf{r}_n^{(\rm opt)}(t);m)$ one should assume that the atoms in clouds 1 and 2 are at their stable equilibrium positions $\mathbf{r}_1(t)$ and

$\mathbf{r}_2(t)$. In other words, there is no fluctuational barrier preparation [32,33] for intercloud switching, even though the switching barrier is strongly affected by the many-body interaction. This significantly simplifies the explicit calculation.

Equation (8) shows that the effective switching activation energy linearly depends on the numbers of atoms in the clouds, for weak interatomic coupling. Even though $|R_n^{(1)}|$ is small compared to the single-atom activation energy $R^{(0)}$, it can largely exceed k_BT, in which case the change of the switching rate will be large. From Eqs. (5) and (8) we obtain Eq. (3) for the many-atom switching rate $W_{12} \equiv W_{12}(N_1;N_{\text{tot}})$, with

$$\alpha = (\alpha_{11} - \alpha_{12})/2k_BT, \quad \beta = -(\alpha_{11} + \alpha_{12})/2k_BT. \tag{9}$$

We have used here the symmetry properties of the parameters α_{nm}; as mentioned below Eq. (3), $W_{21}(N_2;N_{\text{tot}}) = W_{12}(N_2;N_{\text{tot}})$ with the same $N_{\text{tot}}=N_1+N_2$.

In what follows we consider the case $\alpha > 0$, which corresponds to the effective attraction between the clouds. This means that the interaction lowers the barrier for intercloud switching where there are more atoms in the cloud into which the switching occurs.

IV. SYMMETRY-BREAKING TRANSITION

A. Master equation

Because atoms move fast within the clouds compared to the rate of intercloud switching, on time scale $\sim W_{nm}^{-1}$ the state of the system is *fully characterized* by the numbers of atoms in each cloud N_1,N_2. For a given N_{tot}, the system is described by probability $P_1(N_1)$ to have N_1 atoms in cloud 1 at time t. This probability can be found from the master equation

$$\dot{P}_1(N_1) = -[\mu(N_1) + \nu(N_1)]P_1(N_1) + \nu(N_1 - 1)P_1(N_1 - 1) + \mu(N_1 + 1)P_1(N_1 + 1),$$

$$\mu(N_1) = N_1 W_{12}(N_1;N_{\text{tot}}), \quad \nu(N_1) = (N_{\text{tot}} - N_1) \times W_{12}(N_{\text{tot}} - N_1;N_{\text{tot}}). \tag{10}$$

Here we have taken into account that, as a result of a $n \to m$ transition, the number of atoms in cloud n decreases by 1 and in cloud m increases by 1, and that the total probability of such a transition per unit time for N_n atoms in cloud n is $N_n W_{nm}$.

Prior to making a transition the atom will move randomly within the cloud for a long time and will completely "forget" its initial state. It is this randomization that makes the many-particle system zero-dimensional and leads to the mean-field approximation being exact.

The stationary solution of Eq. (10) is

$$P_1^{\text{st}}(N_1) = Z^{-1}\binom{N_{\text{tot}}}{N_1}\exp[-2\alpha N_1(N_{\text{tot}} - N_1)], \tag{11}$$

where $Z \equiv Z(N_{\text{tot}})$ is the normalization constant given by condition $\Sigma_{N_1} P_1(N_1) = 1$.

For large N_{tot}, the function $P_1^{\text{st}}(N_1)$ has one or two sharp peaks. The location of the peak(s) depends on the total number of atoms. We will study the critical region where N_{tot} is close to $1/\alpha$, in which case near the peak(s) $|N_1 - N_2| \ll N_{\text{tot}}$. It is convenient then to introduce a quasicontinuous variable $x = (N_2 - N_1)/N_{\text{tot}} = 1 - 2N_1/N_{\text{tot}}$. For $|x| \ll 1$ from Eq. (11) we find

$$P_1^{\text{st}}(N_1) \approx \tilde{Z}^{-1}\exp[-N_{\text{tot}}(x^4 - 6\theta x^2)/12],$$

$$\theta = \alpha N_{\text{tot}} - 1, \tag{12}$$

where $\tilde{Z}$ is the normalization constant.

Equation (12) has the standard form of the mean-field probability distribution near a symmetry-breaking transition [25]. The parameter θ is the control parameter, which plays the role of the deviation from the critical temperature in systems in thermal equilibrium, whereas x plays the role of the order parameter. Parameter θ linearly depends on the total number of atoms; it also linearly depends on the reciprocal temperature. The critical number of atoms N_c is determined by condition $\theta=0$,

$$N_c = 1/\alpha \propto T. \tag{13}$$

B. Critical exponents

The mean reduced difference of the cloud populations $\eta = \langle x \rangle$ is determined by the position x_0 of the maximum of the distribution $P_1^{\text{st}}(N_1)$. For $\theta < 0$ the distribution has one maximum at $x_0 = \eta = 0$, whereas at $\theta > 0$ it has two symmetric maxima. They are given by equation

$$x_0 = \tanh[(\theta + 1)x_0],$$

which can be obtained from Eq. (11) if one does not limit the analysis to the region $|x| \ll 1$. Close to the critical point

$$\eta = N_{\text{tot}}^{-1}\langle N_2 - N_1 \rangle = \pm (3\theta)^{1/2} \quad \text{for } 0 < \theta \ll 1, \tag{14}$$

which is the familiar mean-field scaling with the critical exponent 1/2. The system occupies one of the states with $|\eta| > 0$, which corresponds to a spontaneous symmetry breaking.

For $1 \gg |\theta| \gg N_c^{-1/2}$, from Eq. (12) we obtain for the variance of the fluctuations of relative populations $\sigma^2 = N_{\text{tot}}^{-2}\langle (N_2 - N_1)^2 \rangle - \eta^2$

$$\sigma^2 = (N_c|\theta|)^{-1} \quad \text{for } \theta < 0;$$

$$\sigma^2 = (2N_c|\theta|)^{-1} \quad \text{for } \theta > 0 \tag{15}$$

($|\theta| \ll 1$). This shows the familiar θ^{-1} scaling of the variance of the order parameter on the both sides of the critical point. At the critical point, $\theta=0$, we have $\sigma^2 = 2\pi\sqrt{6}N_c^{-1/2}/\Gamma(1/4)^2 \approx 1.2N_c^{-1/2}$. Note that $\langle x^2 \rangle$ remains finite in a finite-size system at the critical point, but its dependence on $N_{\text{tot}} \approx N_c$ is given by factor $N_{\text{tot}}^{-1/2}$ instead of N_{tot}^{-1} far from criticality.

C. Response to the symmetry-breaking field

The symmetry of the period-two vibrational states can be lifted if the system is driven by an extra additive force $\mathbf{h}(t)$

$=\mathbf{h}\cos(\omega_F t/2+\phi_h)$. Such force is an analog of a static force in a thermal equilibrium system, it is "static" in the frame oscillating at frequency $\omega_F/2$. In the experiment the force was produced by modulating the counterpropagating laser beams at frequency $\omega_F/2$ with different amplitude; the phase ϕ_h is counted off from the phase of the strong modulation with period τ_F.

Response to a period-$2\tau_F$ force becomes strongly nonlinear at the critical point $\theta=0$ even for small amplitude $|\mathbf{h}|$, because the force modifies the switching activation energies $R_{1,2}$ [24]. In the presence of the force, $R_{1,2}$ can be found from Eq. (6) with $\mathbf{G}\to\mathbf{G}+\mathbf{h}(t)$. Extending the analysis of Refs. [24,30], we obtain to first order in the interatomic interaction and the symmetry-lifting field

$$R_n = R^{(0)} + R_n^{(1)} + R_n^{(h)},$$

$$R_n^{(h)} = -\int dt \boldsymbol{\lambda}_n^{(\mathrm{opt})}(t)\mathbf{h}(t) = \bar{h}\cos\phi_n. \tag{16}$$

The terms $R_{1,2}^{(h)}$ are proportional to the field amplitude, $\bar{h} \propto |\mathbf{h}|$. The phases $\phi_{1,2}$ were obtained earlier for a weakly nonlinear parametrically modulated oscillator [24]. In the general case, $\phi_{1,2}$ are linear in ϕ_h. In addition, $\phi_2=\phi_1+\pi$. The latter relation can be immediately seen from Eq. (16), since by symmetry $\boldsymbol{\lambda}_2^{(\mathrm{opt})}(t)=\boldsymbol{\lambda}_1^{(\mathrm{opt})}(t+\tau_F)$, whereas $\mathbf{h}(t+\tau_F)=-\mathbf{h}(t)$. As a consequence, $R_1^{(h)}=-R_2^{(h)}$.

Even though $|R_n^{(h)}|\ll R^{(0)}$ for small field amplitude $|\mathbf{h}|$, the ratio $R_n^{(h)}/k_BT$ should not be small, and therefore the field-induced change of the switching rates may be substantial. At the same time, the change of the amplitudes of the cloud vibrations remains small for small $\mathbf{h}$ and will not be discussed. Equation (16) for $R_n^{(h)}$ resembles the change of the free energy of an Ising spin by a magnetic field $\propto\bar{h}$ tilted by an angle ϕ_1 with respect to the quantization axis.

The difference in the activation energies $R_{1,2}^{(h)}$ makes the transition rates W_{12} and W_{21} different, as seen from Eq. (5), which in turn lifts the degeneracy of the states 1 and 2 even in the absence of the interatomic coupling. To find the stationary probability distribution in the presence of extra modulation and the interaction, one should multiply the rate coefficients $\mu(N_1)$ and $\nu(N_1)$ in master Eq. (10) by factors $\exp h_{12}$ and $\exp(-h_{12})$, respectively, with

$$h_{12} = -(\bar{h}/k_BT)\cos\phi_1.$$

As a result $P_1^{\mathrm{st}}(N_1)$ acquires an extra factor compared to Eq. (12),

$$P_1^{\mathrm{st}}(N_1) \to P_1^{\mathrm{st}}(N_1)\exp(N_{\mathrm{tot}}xh_{12}) \tag{17}$$

[the normalization constant in P_1^{st} is changed appropriately; we remind that $x=(N_2-N_1)/N_{\mathrm{tot}}$.].

The equation for the maximum of the distribution $x_0=\eta$ near criticality now becomes $\theta x_0-\frac{1}{3}x_0^3+h_{12}=0$. For small $|h_{12}|\ll 1$ and not too close to the phase-transition point, $1\gg|\theta|\gg N_c^{-1/2}$, we have

$$\eta \approx -\theta^{-1}h_{12} \quad (\theta<0),$$

$$\eta \approx \pm(3\theta)^{1/2}+(2\theta)^{-1}h_{12} \quad (\theta>0). \tag{18}$$

The generalized resonant linear susceptibility $\Xi(0)=-d\eta/d\bar{h}$ scales as $|\theta|^{-1}$ on the both sides of the phase-transition point and diverges for $\theta\to 0$. We note that, even though we consider a system far from equilibrium and the susceptibility is calculated with respect to a time-dependent field, for $N_{\mathrm{tot}}=\mathrm{const}$ it is simply related to the variance of the order parameter σ^2 as given by Eq. (15).

At the phase-transition point, $\theta=0$, there is no linear static susceptibility, and $\eta=x_0\propto\bar{h}^{1/3}$, as seen in the experiment.

D. Frequency dispersion of the linear susceptibility

The above analysis can be extended also to the case of an extra additive force with frequency $(\omega_F/2)+\Omega$ that differs from, but remains close to $\omega_F/2$, i.e., $|\Omega|\ll\Gamma\ll\omega_F$. The response to such field should be strong near the symmetry-breaking transition because the system displays large slow fluctuations in this range.

A convenient way of the analysis of the response is based on transforming Eq. (10) for the probability distribution into a Fokker-Planck equation by expanding $P_1(N_1\pm 1)-P_1(N_1)\approx\pm\partial_{N_1}P_1+(1/2)\partial_{N_1}^2P_1$ and using similar expansions for μ,ν [34]. In the absence of extra modulation, for small $x=(N_2-N_1)/N_{\mathrm{tot}}$ to leading order in x the equation reads

$$\tilde{W}^{-1}\dot{P}_1 = \hat{L}P_1, \quad \tilde{W} = W^{(0)}\exp(\beta N_{\mathrm{tot}}),$$

$$\hat{L}P_1 = -2\partial_x\left[\left(\theta x - \frac{1}{3}x^3\right)P_1\right] + 2N_{\mathrm{tot}}^{-1}\partial_x^2 P_1. \tag{19}$$

The stationary solution of Eq. (19) P_1^{st} has the form Eq. (12).

An extra additive force $\mathbf{h}\cos[(\frac{1}{2}\omega_F+\Omega)t]$ with small Ω adiabatically modulates the rates W_{nm} of the intercloud transitions, i.e., one can think of the rates W_{nm} as parametrically dependent on time. The major contribution to the rate modulation comes from the modulation of the activation energies, which is described by Eq. (16) with

$$R_1^{(h)} \equiv R_1^{(h)}(t) = -R_2^{(h)}(t) = \bar{h}\cos(\Omega t); \tag{20}$$

we have disregarded a time-independent phase in the argument of the cosine; it can be eliminated by changing time origin.

For weak modulation one can linearize the transition rates W_{nm} in $\bar{h}$ and consider the terms $\propto\bar{h}$ as a perturbation. Then the distribution can be sought in the form $P_1=P_1^{\mathrm{st}}+\delta P_1$, where the field-induced term $\delta P_1\propto\bar{h}$ is oscillating at frequency Ω. It is given by equation

$$\tilde{W}^{-1}\delta\dot{P}_1 - \hat{L}\delta P_1 = 2\frac{\bar{h}}{k_BT}\cos(\Omega t)N_{\mathrm{tot}}\left(\theta x - \frac{1}{3}x^3\right)P_1^{\mathrm{st}}. \tag{21}$$

Equation (21) allows one to find the periodically oscillating term in the order parameter $\delta\eta(t)=\langle x\rangle-x_0$ (x_0 is the position of the maximum of the distribution for $\bar{h}=0$) and the generalized susceptibility $\Xi(\Omega)$, which can be defined by expression

$$\delta\eta(t) = -\frac{1}{2k_BT}[\Xi(\Omega)\bar{h}\exp(-i\Omega t) + \text{c.c.}].$$

Multiplying Eq. (21) by x, integrating over x, and expanding $\theta x - x^3/3$ in $\hat{L}$ about x_0, for $1 \gg |\theta| \gg N_{\text{tot}}^{-1/2}$ one finds

$$\Xi(\Omega) = 2\tilde{W}/(2|\theta|\tilde{W} - i\Omega), \quad \theta < 0,$$

$$\Xi(\Omega) = 2\tilde{W}/(4\theta\tilde{W} - i\Omega), \quad \theta > 0. \tag{22}$$

[in Eq. (19) for $\tilde{W}$, one should replace N_{tot} with N_c]. For $\Omega \neq 0$ the susceptibility Eq. (22) remains finite even at the phase transition, $\theta=0$. Here $\Xi(\Omega) = 2i\tilde{W}/\Omega$. The susceptibility diverges with frequency, with critical exponent equal to -1.

V. FLUCTUATIONS OF THE TOTAL TRAP POPULATION

In the above analysis we disregarded inelastic collisions between trapped atoms and collisions with atoms outside the trap. These processes lead to fluctuations of the total number of atoms in the trap. In the experimental conditions far from the critical point such fluctuations were slow, with rates an order of magnitude smaller than the rate of intercloud transitions $W^{(0)}$. However, near the critical point intercloud population fluctuations are slowed down, and then fluctuations of the total number of trapped atoms N_{tot} may become important.

In the presence of fluctuations of N_{tot} the state of the system should be characterized by the probability $P(\mathbf{N})$ [$\mathbf{N} \equiv (N_1, N_2)$] to have N_1 atoms in cloud 1 and N_2 atoms in cloud 2, with $N_{\text{tot}} = N_1 + N_2$. For comparatively small N_{tot} and low temperatures used in the experiment, evaporation from the trap due to inelastic collisions between trapped atoms was rare. The major mechanism of the change of N_{tot} was collisions with atoms outside the trap. In a simple model of such collisions, the rate of loss of atoms from an nth cloud $W_{\text{out}}N_n$ is proportional to the number of atoms in the cloud N_n, whereas the rate of capture of outside atoms by a cloud $W_{\text{out}}N_0/2$ is independent of N_n and depends only on the density of outside atoms (which determines N_0) and the cross-section of their capture. We disregard fluctuations in the density of outside atoms and choose parameter N_0 in such a way that it provides the typical scale of N_{tot}, as will be seen below.

A. Fokker-Planck equation near criticality

The master equation for $P(\mathbf{N})$ can be written as a direct extension of Eq. (10),

$$\dot{P}(\mathbf{N}) = \tilde{W}\hat{L}_{\text{cl}}P + W_{\text{out}}\hat{L}_{\text{out}}P, \quad \hat{L}_{\text{cl}}P = -\sum_n \mu'(N_n; N_{\text{tot}})P(\mathbf{N})$$
$$+ \mu'(N_1+1; N_{\text{tot}})P(N_1+1, N_2-1)$$
$$+ \mu'(N_2+1; N_{\text{tot}})P(N_1-1, N_2+1),$$

$$\hat{L}_{\text{out}}P = -(N_1+N_2+N_0)P(\mathbf{N}) + \sum_n (N_n+1)P(\mathbf{N}+\boldsymbol{\delta}_n)$$
$$+ (N_0/2)\sum_n P(\mathbf{N}-\boldsymbol{\delta}_n), \tag{23}$$

where

$$\mu'(N_n; N_{\text{tot}}) = N_n \exp(\alpha N_{\text{tot}} - 2\alpha N_n) \equiv \tilde{W}^{-1}\mu(N_n),$$

$\boldsymbol{\delta}_1 = (1,0)$, and $\boldsymbol{\delta}_2 = (0,1)$ [the intercloud switching rate $\tilde{W}$ is defined in Eqs. (3) and (19)]. The terms $\hat{L}_{\text{cl}}$ and $\hat{L}_{\text{out}}$ describe intercloud transitions and atom exchange with the surrounding, respectively. We assume that the typical rate of the exchange is $W_{\text{out}} \ll \tilde{W}$.

We now consider the critical region where N_{tot} is close to N_c. We will be interested in the range of N_1, N_2 where $P(N_1, N_2)$ is close to maximum, $|N_1 - N_2| \ll N_{\text{tot}}$, and introduce quasicontinuous variables

$$x = \frac{N_2 - N_1}{N_0}, \quad u = \frac{N_1 + N_2}{N_0} - 1,$$

$$\theta = \alpha N_0 - 1. \tag{24}$$

As we will see, variables x and θ coincide with the variables used earlier if fluctuations of the total number of trapped atoms can be disregarded; variable u gives the deviation of N_{tot} from N_0.

For $|x| \ll 1$, $|\theta| \ll 1$, and $|u| \ll 1$ to leading order in x, θ, u, and N_0^{-1} the operators $\hat{L}_{\text{cl}}$ and $\hat{L}_{\text{out}}$ become

$$\hat{L}_{\text{cl}}P = -2\partial_x\left\{\left[x(\theta+u) - \frac{1}{3}x^3\right]P\right\} + 2N_0^{-1}\partial_x^2 P,$$

$$\hat{L}_{\text{out}}P = \partial_x(xP) + \partial_u(uP) + N_0^{-1}[(\partial_x^2 + \partial_u^2)P]. \tag{25}$$

Equations (23)–(25) allow one to study the stationary distribution of the modulated system in the presence of fluctuations of the total population. We note first that exchange of atoms with the surrounding leads to effective exchange of atoms between the clouds. In turn, this leads to renormalization of intercloud transition rates and, effectively, of the control parameter, which can be found from Eq. (25) by looking at the terms $\propto \partial_x(xP)$.

$$\theta \to \theta - \frac{W_{\text{out}}}{2\tilde{W}}, \quad N_c \to \alpha^{-1}\left(1 + \frac{W_{\text{out}}}{2\tilde{W}}\right). \tag{26}$$

The change of θ is negative, which should be expected, since exchange with the surrounding should stabilize the symmetric phase, and therefore a larger number of atoms is required for the symmetry-breaking transition than in the case where there is no such exchange.

The parameter N_c in Eq. (26) is the critical value of the parameter N_0. The mean number of trapped atoms is $\langle N_{\text{tot}}\rangle = N_0(1+\langle u\rangle)$. The scaled coefficient of diffusion over x is also renormalized, $2N_0^{-1} \to 2N_0^{-1}(1 + W_{\text{out}}/2\tilde{W})$.

In the stationary regime fluctuations of the total number of atoms in the trap are small, $\langle u^2\rangle \sim 1/N_0$. However, the distribution over the scaled difference of the cloud populations x differs from the standard Landau-type distribution [Eq. (12)]. This is in spite the fact that the system is described by the mean-field theory, no spatial correlations are involved.

The dynamics of x and u are very different. There is no critical slowing down for u, and in the critical region $|\theta| \lesssim N_c^{-1/2}$ the width of the distribution over x is $\sim N_c^{-1/4} \gg N_c^{-1/2}$.

B. Variance of the order parameter

The major effect of the coupling between fluctuations of x and u is the change of the variance $\sigma^2 = \langle x^2\rangle - \langle x\rangle^2$. The latter occurs in the broken-symmetry state where $\theta \gg N_c^{-1/2}$. It can be calculated in the stationary regime by decoupling the chain of equations for the moments of the stationary distribution $\langle x^k u^l\rangle$ with integer k,l. For $N_c^{-1/2} \ll \theta \ll 1$

$$N_c\sigma^2 \approx \frac{1}{2\theta} + \frac{3}{4\theta + (W_{\rm out}/\tilde{W})}. \qquad (27)$$

Fluctuations of u and x (i.e., of the total population of the clouds and the population difference) are correlated in the broken-symmetry phase, with $\langle u(x-x_0)\rangle \approx (2x_0/N_c)[4\theta + (W_{\rm out}/\tilde{W})]^{-1}$, where $x_0 = \pm(3\theta)^{1/2}$.

In contrast, in the symmetric phase fluctuations of u and x are uncorrelated; for $1 \gg -\theta \gg N_c^{-1/2}$

$$N_c\sigma^2 \approx |\theta|^{-1}[1 + (W_{\rm out}/2\tilde{W})] \approx |\theta|^{-1}. \qquad (28)$$

It is seen from Eq. (27) that, for $\theta \gg W_{\rm out}/4\tilde{W}$, the variance of the order parameter fluctuations in the broken-symmetry state scales with the control parameter in the same way as without fluctuations of the total population, $N_c\sigma^2 \approx 5/4\theta$. However, the factor in front of $1/\theta$ is now larger than in the symmetric phase, Eq. (28). This corresponds to what was seen in the experiment.

In the broken-symmetry state, as θ decreases below $W_{\rm out}/4\tilde{W}$, there occurs a crossover to $\sigma^2 \approx 1/2N_c\theta$, i.e., σ^2 scales with θ with the same scaling exponent, but with smaller amplitude than in the symmetric phase. This regime apparently could not be accessed in the experiment.

We note that there are other fluctuations that can contribute to the variance σ^2. For example, slow fluctuations of the trap parameters may lead to small and slow fluctuations of the total population, which can be thought of as fluctuations of the control parameter θ. They give an extra contribution $3\langle(\delta\theta)^2\rangle/4\langle\theta\rangle$ to σ^2 in Eq. (15) for the broken-symmetry phase, where $\langle\delta\theta^2\rangle$ is the variance of θ. Interestingly, this contribution also scales as θ^{-1} away from the critical point. It further increases the difference between the variance of the order parameter in the broken-symmetry and symmetric phase.

VI. ONE-DIMENSIONAL MODEL

A. Rotating wave approximation

The calculation of the switching rates and response coefficients is simplified if the atomic motion in MOT is assumed one-dimensional, along the MOT axis z. This corresponds to averaging over the motion transverse to the axis, which is largely small-amplitude fluctuations about the vibrating centers of the clouds. In the experiment the radiation that confined the atoms transverse to the axis had large intensity, so that the correlation time of these fluctuations was short.

In the single-atom approximation the atomic motion can be modeled by the Duffing oscillator,

$$\ddot{z} + 2\Gamma\dot{z} + \omega_0^2(1 + \epsilon_F \cos \omega_F t)z + \gamma z^3 = f(t)/m_a, \qquad (29)$$

Here, ω_0 and Γ are the MOT eigenfrequency and viscous friction coefficient, respectively, γ is the nonlinearity parameter, and ϵ_F is determined by the amplitude of the laser beam modulation [35]. In the experiment $\gamma = 1.5\times10^5$ s^{-2} cm^{-2} and $\epsilon_F = 0.9$; the values of ω_0 and Γ were given in Sec. II. The nonlinear in the velocity terms, which are disregarded in Eq. (29), are comparatively small for the experimental conditions. The function $f(t)$ is white thermal Gaussian noise.

For the reduced modulation strength $\epsilon_F\omega_0/4\Gamma > 1$, resonant modulation ($|\omega_F - 2\omega_0| \ll \omega_0$) can excite period-two atomic vibrations [36]. The vibrations are nearly sinusoidal in the absence of noise, if the modulation is not too strong. The atomic dynamics can be conveniently described by switching to the rotating frame using a standard transformation

$$z = C_{\rm RWA}[q_2 \cos(\omega_F t/2) - q_1 \sin(\omega_F t/2)],$$

$$\dot{z} = -C_{\rm RWA}(\omega_F/2)[q_2 \sin(\omega_F t/2) + q_1 \cos(\omega_F t/2)], \quad (30)$$

with $C_{\rm RWA} = (2\omega_0^2\epsilon_F/3\gamma)^{1/2}$ (the modulation phase is chosen in such a way that $\epsilon_F/\gamma > 0$). In the rotating wave approximation (RWA), the equations for slow variables $\mathbf{q} \equiv (q_1, q_2)$ in slow time τ are

$$\frac{d\mathbf{q}}{d\tau} = \mathbf{K}(\mathbf{q}) + \mathbf{f}'(\tau), \qquad \tau = \omega_0\epsilon_F t/4. \qquad (31)$$

Here, $\mathbf{f}'(\tau)$ is white Gaussian noise with two asymptotically independent components,

$$\langle f'_\varkappa(\tau) f'_{\varkappa'}(\tau')\rangle = 2D_\tau k_B T \delta_{\varkappa\varkappa'}\delta(\tau - \tau'),$$

$$D_\tau = 6\gamma\Gamma/m_a\omega_0^5\epsilon_F^2 \quad (\varkappa, \varkappa' = 1,2).$$

We use vector notations here *formally*, $\mathbf{q}$ is not a vector in real space, its components are combinations of atomic displacement and momentum along the MOT axis.

Functions $\mathbf{K}(\mathbf{q})$ are cubic polynomials and are given explicitly in Ref. [24]. [they were denoted by $\mathbf{K}^{(0)}(\mathbf{q})$]. The zeros of $\mathbf{K}$ occur at the stationary states in the rotating frame. They correspond to the period-two vibrational states in the laboratory frame. We will be interested in the parameter range where Eq. (31) has two attractors $\mathbf{q}_1^A = -\mathbf{q}_2^A$. Functions $\mathbf{K}$ are also equal to zero for $\mathbf{q} = \mathbf{0}$, which corresponds to the unstable state of zero-amplitude period-two vibrations in the laboratory frame.

For low temperatures, the motion described by Eq. (31) is primarily small-amplitude fluctuations about states $\mathbf{q}_{1,2}^A$. Switching between the states requires a large fluctuation. The single-atom switching rate has the form Eq. (2), with activation energy $R^{(0)}=\min \mathcal{R}^{(0)}$,

$$\mathcal{R}^{(0)} = (4D_\tau)^{-1}\int d\tau \mathbf{f}'^2(\tau) + \int d\tau \boldsymbol{\lambda}(\tau)\left[\frac{d\mathbf{q}}{d\tau} - \mathbf{K} - \mathbf{f}'(\tau)\right]. \tag{32}$$

The major distinction from the general formulation [Eq. (6)] is that function $\mathbf{K}$ does not explicitly depend on time. This significantly simplifies the variational problem [Eq. (32)]. The corresponding optimal trajectories followed in switching from nth stable state $\mathbf{q}_n^{(\mathrm{opt})}(\tau)$ were found in Ref. [16], whereas functions $\boldsymbol{\lambda}_n^{(\mathrm{opt})}(\tau)$ are equal to the logarithmic susceptibilities found in Ref. [24] multiplied by $-1/D_\tau$.

B. Interatomic interaction

The major interatomic interaction that affects the switching rate is the long-range interaction, since in switching atoms move far away from the clouds. It comes from the shadow effect, which is due to "shielding" of atoms from the laser light by other atoms [3,4,21–23]. In the one-dimensional picture, the force on ith atom with coordinate z^i from other atoms can be approximately modeled as $F^i = -f_{\mathrm{sh}}\Sigma_j \mathrm{sgn}(z^i - z^j)$. This force is weak, much smaller than the Doppler force that confines atoms to the trap. Multiple scattering of light is disregarded in the above expression.

To estimate f_{sh} for a switching atom we have to take into account that the atomic clouds are three-dimensional. We consider a simple model in which a laser beam propagating along z-axis passes on its way through an atomic cloud with density distribution $\rho(\mathbf{r})$. The resulting change of the beam intensity I as a function of transverse coordinates x,y is $\Delta I(x,y) = I\sigma_L \int dz \rho(\mathbf{r})$, where integration is done over the length of the cloud and σ_L is the absorption cross-section. This cross-section depends in the standard way on intensity I and the frequency detuning. Generally, because of the magnetic-field induced frequency shift and the Doppler shift, σ_L oscillates in time. The light intensity also oscillates in time. If we disregard these oscillations, we get for typical experimental conditions $\sigma_L \approx 5.6\times 10^{-15}$ m^2.

The atomic density distribution $\rho(\mathbf{r})$ can be assumed Gaussian with the same width $w_t \approx 1$ mm in all directions, which was achieved in the experiment by tuning the transverse beam intensities. According to the optimal path picture, during switching atoms most likely move along the MOT axis, and for such atoms the light intensity change is determined by $\rho(\mathbf{r})$ on the axis. The extra force on the switching atom as it moves between the clouds is then directed toward the more populated cloud and is equal to $f_{\mathrm{sh}}|N_1 - N_2|$ where, according to the above arguments,

$$f_{\mathrm{sh}} = \hbar k \Gamma_p \sigma_L s / 4\pi (s+1) w_t^2. \tag{33}$$

Here, k is the photon wave number, Γ_p is the reciprocal lifetime of the excited state, and $s = (I/I_s)[1+(2\delta/\Gamma_p)^2]^{-1}$ is the resonant absorption strength (I_s is the saturation intensity and δ is the detuning of the radiation frequency from the atomic transition frequency). Equation (33) gives $f_{\mathrm{sh}} \approx 2.5 \times 10^{-32}$ N. Note that, since the clouds are oscillating, the force $\propto f_{sh}$ is oscillating as well, its time dependence is determined by the sgn-function.

C. Shadow effect in the rotating frame

The effect of the shadow force in the many-atomic system can be conveniently analyzed in the rotating frame by changing from coordinates and momenta $(z^i, \dot{z}^i)$ to slowly varying two-component vectors $\mathbf{q}^i$, Eq. (30) (superscript i enumerates the atoms). In the RWA the equation of motion for $\mathbf{q}^i$ becomes

$$\frac{d\mathbf{q}^i}{d\tau} = \mathbf{K}^i(\mathbf{q}^i) + \hat{\epsilon}\partial_{\mathbf{q}^i} H_{\mathrm{sh}} + \mathbf{f}'^i(\tau) \tag{34}$$

with $i=1,\ldots,N_{\mathrm{tot}}$. Here, $\mathbf{f}'^i(\tau)$ is the random force on ith atom (random forces on different atoms are uncorrelated), $\hat{\epsilon}$ is the permutation tensor, and H_{sh} is the interaction Hamiltonian in the slow variables,

$$H_{\mathrm{sh}} = \frac{1}{2}\sum_{ij}{}' V_{\mathrm{sh}}(\mathbf{q}^i - \mathbf{q}^j),$$

$$V_{\mathrm{sh}}(\mathbf{q}) = \frac{8 f_{\mathrm{sh}}}{\pi m_a \omega_0^2 \epsilon_F C_{\mathrm{RWA}}}|\mathbf{q}|, \tag{35}$$

where the prime indicates that $i \neq j$.

In the RWA, the coefficients α_{nm} in the expression for the interaction-induced correction to the switching activation energy R_n, Eq. (8), are

$$\alpha_{nm} = \int_{-\infty}^{\infty} d\tau \boldsymbol{\lambda}_n^{(\mathrm{opt})}(\tau)\hat{\epsilon}\partial_{\mathbf{q}_m^A} V_{\mathrm{sh}}(\mathbf{q}_n^{(\mathrm{opt})}(\tau) - \mathbf{q}_m^A), \tag{36}$$

where $\boldsymbol{\lambda}_n^{(\mathrm{opt})}(\tau)$ and $\mathbf{q}_n^{(\mathrm{opt})}(\tau)$ are the solutions of the single-atom problem of minimizing the functional (32) for switching from the state n.

Equations (32) and (36) were used to find the coefficients α_{nm} and the critical value of the total number of atoms $N_c = 2k_B T/(\alpha_{11} - \alpha_{12})$ where the symmetry-breaking transition occurs. The obtained N_c was within a factor of 2 from the value of N_c observed in the experiment. This is reasonable given the uncertainty in the temperature, the renormalization of N_c by the finite lifetime of atoms in the MOT, cf. Eq. (26), and most importantly, the fact that the light intensity modulation was not weak and, respectively, the atomic vibrations noticeably deviated from sinusoidal.

Change of the vibration amplitude due to the atom-atom coupling

An important effect that allows one to compare independently the many-atomic theory with the experiment is the change of the vibration amplitudes due to the interaction. It is determined by the change of the equilibrium positions $\mathbf{q}_n^A$ in the rotating frame. For weak interatomic interaction it can be found by linearizing equations of motion [Eq. (34)]. The average force on an atom from other atoms in the same cloud is equal to zero. The shift of the equilibrium position is due only to the force from the atoms in the other cloud. Disregarding small fluctuations about the equilibrium positions, for the shift of nth attractor in the rotating frame $\delta\mathbf{q}_n^A$ we obtain

$$(\delta\mathbf{q}_n^A\partial_{\mathbf{q}_n^A})\mathbf{K}(\mathbf{q}_n^A) + N_{3-n}\hat{\epsilon}\partial_{\mathbf{q}_n^A}\bar{V}_{\mathrm{sh}}(\mathbf{q}_n^A - \mathbf{q}_{3-n}^A) = 0. \qquad (37)$$

Here, $\bar{V}_{\mathrm{sh}}$ is given by Eq. (35) for V_{sh} in which f_{sh} is replaced with $\bar{f}_{\mathrm{sh}}$. The quantity $\bar{f}_{\mathrm{sh}}$ characterizes the force from the shadow effect which is averaged over the cross section of the cloud transverse to the MOT axis. Such averaging occurs as atoms are moving within the cloud. If the density distributions within the clouds are Gaussian with the same width, $\bar{f}_{\mathrm{sh}}=f_{\mathrm{sh}}/2$.

The shift of the nth attractor $(n=1,2)$ given by Eq. (37) and the corresponding change of the vibration amplitude of the nth cloud is proportional to the number of atoms in the other cloud, N_{3-n}. Therefore the vibration amplitudes of the clouds become different in the broken-symmetry state. This prediction and the linear dependence of the amplitude change on the number of atoms in the other cloud are in full agreement with the experiment; the numerical estimate for the simplified model of sinusoidal 1D vibrations is within a factor of 2 from the measured value.

VII. CONCLUSIONS

We have observed and explained an ideal mean-field transition far from equilibrium, the spontaneous breaking of the discrete time-translation symmetry. The transition occurs in a system of periodically modulated trapped atoms. The mean-field behavior is evidenced by the critical exponents of the order parameter and its variance, the nonlinear resonant response at criticality, and the linear susceptibility as a function of the distance to the critical point.

The proposed theory explains the symmetry-breaking transition as resulting from the interplay of the atom-atom interaction and the nonequilibrium fluctuations. Both components are necessary. The fluctuations, even though they are small on average, cause transitions between the period-two states of atomic vibrations in the modulated trap, i.e., between the two vibrating atomic clouds. The interaction, which is also small and only slightly affects the vibrational states, is nevertheless strong enough to compete with the small-intensity fluctuations and thus change the switching rates.

In contrast to conventional phase transitions, in our system the control parameter θ is not intensive (as temperature, for example), it linearly depends on the total number of atoms N_{tot}. The transition is a many-body effect, but even though the system is large, with $\sim 10^7$ atoms, it is finite. Once the time-translation symmetry is broken with increasing N_{tot}, a further increase of N_{tot} should not change the symmetry as long as the trap remains stable. We note that the critical value of N_{tot} is proportional to temperature.

The ideal mean-field behavior in the many-atom system is a result of the time scale separation. The intercloud transitions are rare, the transition rate is small compared to the decay rate and the vibration frequency. This means that the intracloud fluctuations have a short correlation time compared to the intercloud fluctuations and the behavior of the system is controlled by the difference in the number of atoms in the vibrating clouds. The proposed theory is in full agreement with the observations.

ACKNOWLEDGMENTS

We thank M. C. Cross, G. S. Jeon, W. D. Phillips, D. L. Stein, and T. G. Walker for helpful comments. This work was supported by the Acceleration Research Program of Korean Ministry of Science and Technology. M.D. was supported in part by NSF Grant No. PHY-0555346. WJ acknowledges support from Yeonam Foundation.

[1] L. Kadanoff, J. Stat. Phys. **137**, 777 (2009).
[2] M. Cross and H. Greenside, *Pattern Formation and Dynamics in Nonequilibrium Systems* (Cambridge University Press, Cambridge, England, 2009).
[3] T. Walker, D. Sesko, and C. Wieman, Phys. Rev. Lett. **64**, 408 (1990).
[4] D. W. Sesko, T. G. Walker, and C. E. Wieman, J. Opt. Soc. Am. B **8**, 946 (1991).
[5] K. Kim, H. R. Noh, Y. H. Yeon, and W. Jhe, Phys. Rev. A **68**, 031403 (2003).
[6] K. L. Turner, S. A. Miller, P. G. Hartwell, N. C. MacDonald, S. H. Strogatz, and S. G. Adams, Nature (London) **396**, 149 (1998).
[7] E. Buks and M. L. Roukes, J. Microelectromech. Syst. **11**, 802 (2002).
[8] H. B. Chan and C. Stambaugh, Phys. Rev. Lett. **99**, 060601 (2007).
[9] R. Lifshitz and M. C. Cross, Phys. Rev. B **67**, 134302 (2003).
[10] K. Kim, M. S. Heo, K. H. Lee, K. Jang, H. R. Noh, D. Kim, and W. Jhe, Phys. Rev. Lett. **96**, 150601 (2006).
[11] M. H. Anderson, J. R. Ensher, M. R. Matthews, C. E. Wieman, and E. A. Cornell, Science **269**, 198 (1995).
[12] K. B. Davis, M. O. Mewes, M. R. Andrews, N. J. van Druten, D. S. Durfee, D. M. Kurn, and W. Ketterle, Phys. Rev. Lett. **75**, 3969 (1995).
[13] K. Damle, T. Senthil, S. N. Majumdar, and S. Sachdev, EPL **36**, 7 (1996).
[14] Q. Niu, I. Carusotto, and A. B. Kuklov, Phys. Rev. A **73**, 053604 (2006).
[15] T. Donner, S. Ritter, T. Bourdel, A. Ottl, M. Kohl, and T. Esslinger, Science **315**, 1556 (2007).
[16] M. I. Dykman, C. M. Maloney, V. N. Smelyanskiy, and M. Silverstein, Phys. Rev. E **57**, 5202 (1998).
[17] L. J. Lapidus, D. Enzer, and G. Gabrielse, Phys. Rev. Lett. **83**, 899 (1999).
[18] I. Siddiqi, R. Vijay, F. Pierre, C. M. Wilson, M. Metcalfe, C.

Rigetti, L. Frunzio, and M. H. Devoret, Phys. Rev. Lett. **93**, 207002 (2004).

[19] R. Vijay, M. H. Devoret, and I. Siddiqi, Rev. Sci. Instrum. **80**, 111101 (2009).

[20] J. S. Aldridge and A. N. Cleland, Phys. Rev. Lett. **94**, 156403 (2005).

[21] J. Dalibard, Opt. Commun. **68**, 203 (1988).

[22] J. T. Mendonça, R. Kaiser, H. Terças, and J. Loureiro, Phys. Rev. A **78**, 013408 (2008).

[23] A. M. Steane, M. Chowdhury, and C. J. Foot, J. Opt. Soc. Am. B **9**, 2142 (1992).

[24] D. Ryvkine and M. I. Dykman, Phys. Rev. E **74**, 061118 (2006).

[25] L. Landau and E. M. Lifshitz, *Statistical Physics. Part 1*, 3rd ed. (Pergamon Press, New York, 1980).

[26] A. S. Arnold and P. J. Manson, J. Opt. Soc. Am. B **17**, 497 (2000).

[27] M. I. Freidlin and A. D. Wentzell, *Random Perturbations of Dynamical Systems*, 2nd ed. (Springer-Verlag, New York, 1998).

[28] M. I. Dykman, Phys. Rev. A **42**, 2020 (1990).

[29] R. P. Feynman and A. R. Hibbs, *Quantum Mechanics and Path Integrals* (McGraw-Hill, New York, 1965).

[30] M. I. Dykman, B. Golding, L. I. McCann, V. N. Smelyanskiy, D. G. Luchinsky, R. Mannella, and P. V. E. McClintock, Chaos **11**, 587 (2001).

[31] H. B. Chan, M. I. Dykman, and C. Stambaugh, Phys. Rev. Lett. **100**, 130602 (2008).

[32] Y. Kagan and M. I. Klinger, Zh. Eksp. Teor. Fiz. **70**, 255 (1976).

[33] Y. Kagan, J. Low Temp. Phys. **87**, 525 (1992).

[34] N. G. Van Kampen, *Stochastic Processes in Physics and Chemistry*, 3rd ed. (Elsevier, Amsterdam, 2007).

[35] K. Kim, H. R. Noh, and W. Jhe, Phys. Rev. A **71**, 033413 (2005).

[36] L. D. Landau and E. M. Lifshitz, *Mechanics*, 3rd ed. (Elsevier, Amsterdam, 2004).